Supporting Information

Regulating steric hindrances of perylenediimide to construct NIR photothermal J-aggregates with large red-shift

Bingcheng Zhou, Hongtao Chen, Chendong Ji* and Meizhen Yin*

State Key Laboratory of Chemical Resource Engineering, Beijing Lab of Biomedical Materials, Beijing University of Chemical Technology, Beijing 100029, China

Contents

1. Materials and instruments

Materials. 1,7-dibromo-3,4,9,10-perylenetetracarboxylic acid dianhydride (PDA-2Br, Hunan Hua Teng), DSPE - PEG (2 KDa, Ponsure Biotechnology, 95%) were used without further purification. Deionized (DI) water (18.2 MΩ·cm resistivity at 25 °C) was prepared through a Millipore Milli-Q purification system. Phosphate buffer solution (PBS), Cell counting kit (CCK-8), Calcein-AM and Propidium iodide (PI) chromophore stuff were purchased from Solarbio. Other reagents were purchased from local commercial suppliers and used without further purification.

Instruments. Nuclear magnetic resonance (NMR) spectra were recorded on a Bruker 400 spectrometer at room temperature. Mass spectra (MS) were measured with a mass spectrometer (Waters, Xevo G2 Qtof, USA). Scanning electron microscopy (SEM, JSM-7500F) and Zetasizer Nano ZS (Brookhaven, Omni, USA) were used to determine the morphology, size, and Zeta potential of PDIA-NPs. UV-vis-NIR absorbance spectra were recorded using a spectrophotometer (UV-2600, Shimadzu, Japan) in a quartz cuvette. The fluorescence spectra were measured using a fluorescence spectrophotometer (Horiba Jobin Yvon FluoroMax-4 NIR, NJ, USA). Photothermal conversion experiments were performed with the following process: the 808 nm laser was employed to irradiate the solution at a power density of 1.0 W/cm^2, and the temperature elevation of the solution was measured in real-time. Cell level FL imaging was measured via EVOS™ FL Imaging System.

2. Synthesis and characterization

The synthetic route of PDIA, PDIB, and PDIC is shown in Scheme S1.

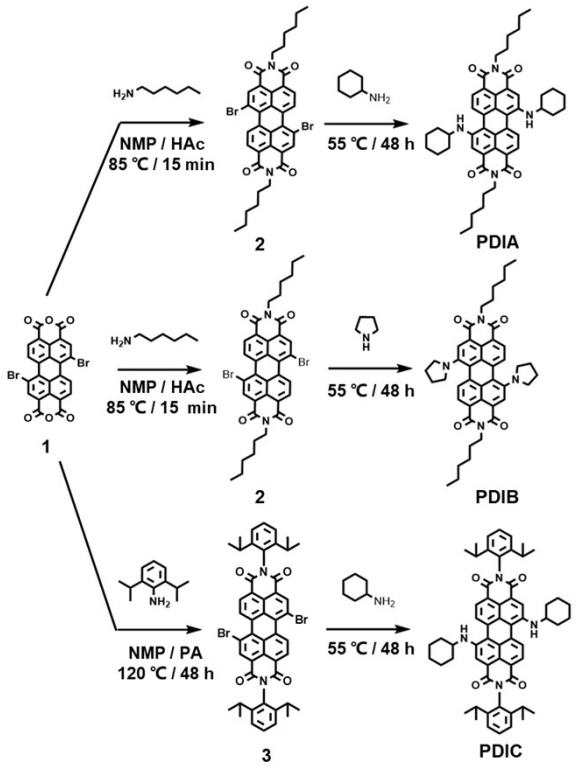

Scheme S1 Synthesis of PDIA, PDIB, and PDIC.

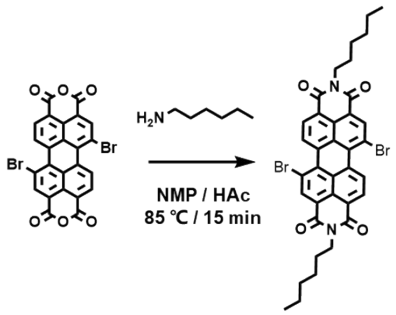

1 2

Synthesis of 2: Compound **1** (1 g, 1.8 mmol), hexylamine (2 mL, 26.2 mmol), and acetic acid (5 mL) was stirred for 15 min at 85 °C. After cooling to room temperature, the solvents were evaporated under reduced pressure. The product was purified by silica gel column chromatography and preparative thin layer chromatography (TLC) (Solvent system: dichloromethane/n-hexane 75/25) to yield red powder, compound **2**. ^{1}H NMR (400 MHz, $CDCl_3$) δ 9.47 (d, 2H), 8.90 (s, 2H), 8.69 (d, 2H), 4.20 (t, 4H), 1.75 (m, 4H), 1.36 (s, 12H), 0.91 (t, 6H).

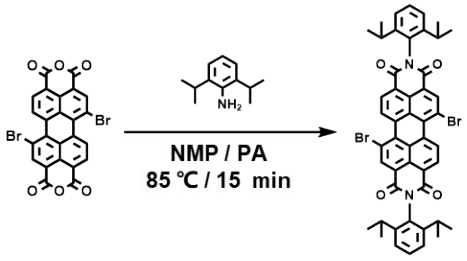

1 3

Synthesis of 3: Compound **1** (1 g, 1.8 mmol), 2,6-diisopropylaniline (4 mL, 21.2 mmol), and propionic acid (250 mL) were stirred for 48 h at 130 °C. After cooling to room temperature, the solid precipitate was washed with water, filtered, and dried. The product was purified by silica gel column chromatography and preparative TLC (Solvent system: dichloromethane/n-hexane 70/30) to yield red powder, compound **3**. ^{1}H NMR (400 MHz, $CDCl_3$) δ 9.56 (d, 2H), 9.02 (s, 2H), 8.82 (d, 2H), 7.52 (t, 2H), 7.38 (d, 4H), 2.76 (m, 4H), 1.20 (d, 24H).

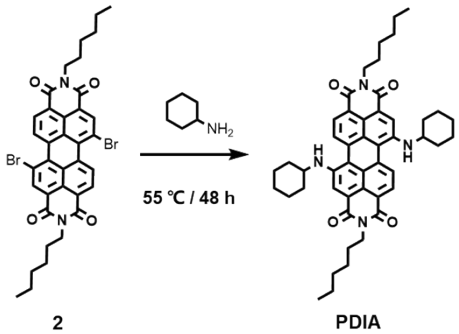

2 PDIA

Synthesis of PDIA: Compound **2** (200 mg, 0.3 mmol) and cyclohexylamine (10 mL, 131 mmol) was stirred for 48 h at 55 °C. After cooling to room temperature, the solvents were evaporated under reduced pressure. The product was purified by silica gel column chromatography and preparative TLC (Solvent system: dichloromethane/n-hexane 70/30) to yield green powder, compound PDIA. Mass spectrum (m/z) Calc. for $C_{48}H_{55}N_4O_4^-$: 751.4302,

found: 751.4250. ^{1}H NMR (400 MHz, $CDCl_3$) δ 8.57 (d, *J* = 80.2 Hz, 2H), 8.31 (d, *J* = 80.4 Hz, 2H), 7.92 (s, *J* = 50.4 Hz, 2H), 4.14 (t, 4H), 3.55 (s, *J* = 100.7 Hz, 2H), 2.06 (m, *J* = 43.2 Hz, 4H), 1.75 (m, 10H), 1.35 (m, 22H), 0.91 (t, 6H).

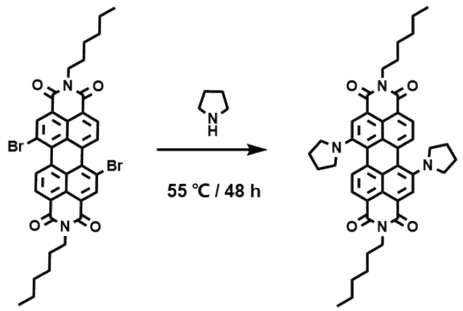

2 PDIB

Synthesis of PDIB: A mixture of compound **2** (200 mg, 0.3 mmol) and pyrrolidine (5 mL, 68.2 mmol) was stirred for 48 h at 55 °C. After cooling to room temperature, the solvents were evaporated under reduced pressure. The product was purified by silica gel column chromatography and preparative TLC (Solvent system: dichloromethane/n-hexane 60/40) to yield green powder, compound PDIB. Mass spectrum (m/z) Calc. for $C_{44}H_{48}N_4O_4$: 696.3676, found: 696.3715. ^{1}H NMR (400 MHz, $CDCl_3$) δ 8.28 (s, 2H), 8.20 (d, 2H), 7.37 (d, 2H), 4.20 (t, 4H), 3.62 (s, 4H), 2.68 (s, 4H), 1.99 (m, 8H), 1.75 (m, 4H), 1.40 (m, *J* = 43.3 Hz, 12H), 0.89 (t, 6H).

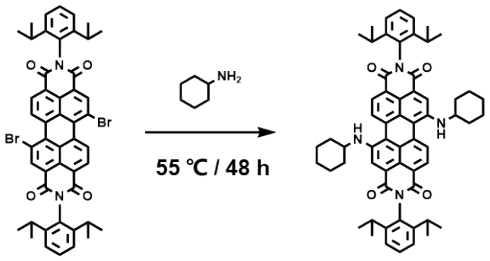

3 PDIC

Synthesis of PDIC: A mixture of compound **3** (200 mg, 0.126 mmol) and cyclohexylamine (10 mL, 131 mmol) was stirred for 48 h at 55 °C. After cooling to room temperature, the solvents were evaporated under reduced pressure. The product was purified by silica gel column chromatography and preparative TLC (Solvent system: dichloromethane/n-hexane 60/40) to yield green powder, compound PDIC. Mass spectrum (m/z) Calc. for $C_{60}H_{63}N_4O_4^-$: 903.4928, found: 903.4846. ^{1}H NMR (400 MHz, $CDCl_3$) δ 8.80 (d, *J* = 65.6 Hz, 2H), 8.56 (d, *J* = 101.3 Hz, 2H), 8.13 (s, *J* = 122.5 Hz, 2H), 7.49 (t, 2H), 7.35 (d, 4H), 3.79 (m, 2H), 2.77 (m, 4H), 2.09 (m, *J* = 59.0 Hz, 4H), 1.82 (m, 4H), 1.59 (m, *J* = 71.0 Hz, 12H), 1.19 (d, 24H).

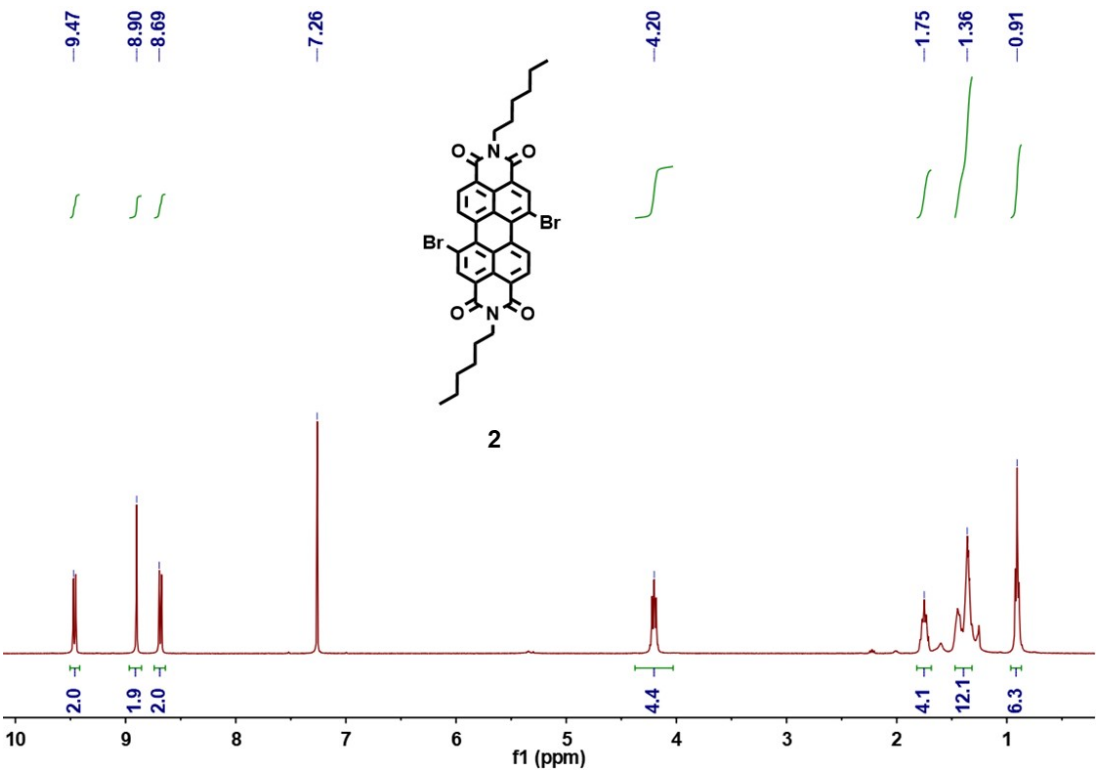

Fig. S1 ^{1}H NMR spectrum of compound **2** in $CDCl_3$.

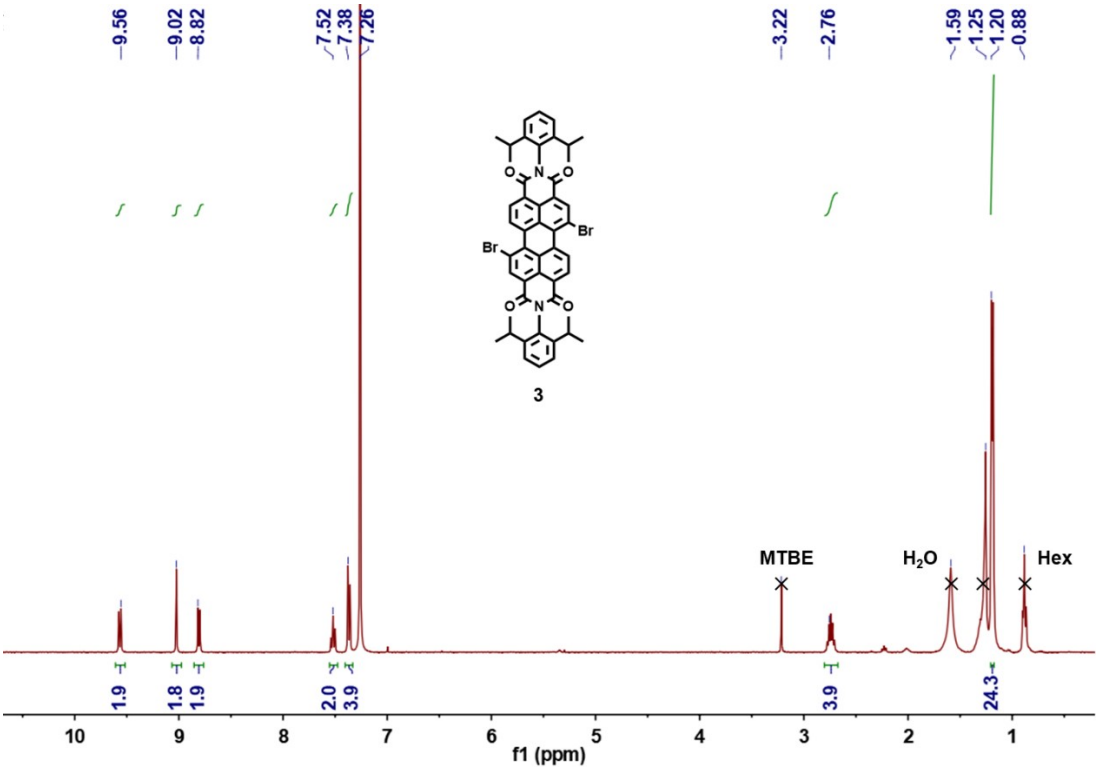

Fig. S2 ^{1}H NMR spectrum of compound **3** in $CDCl_3$.

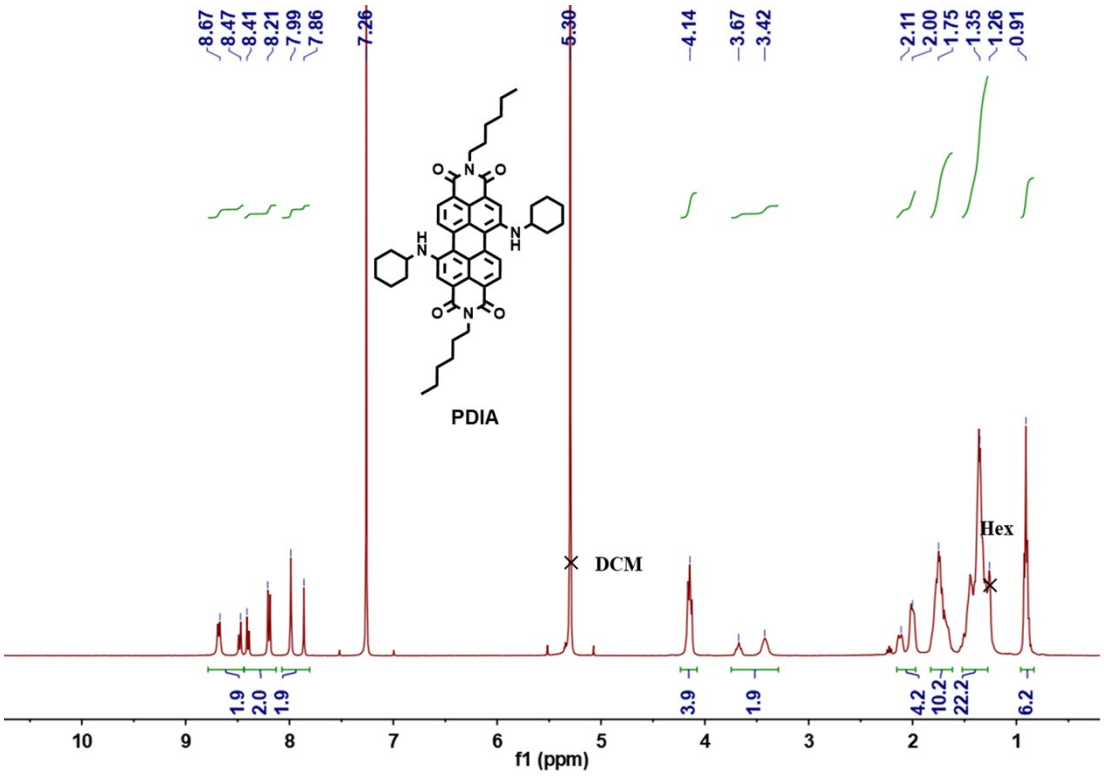

Fig. S3 ^{1}H NMR spectrum of compound **PDIA** in $CDCl_3$.

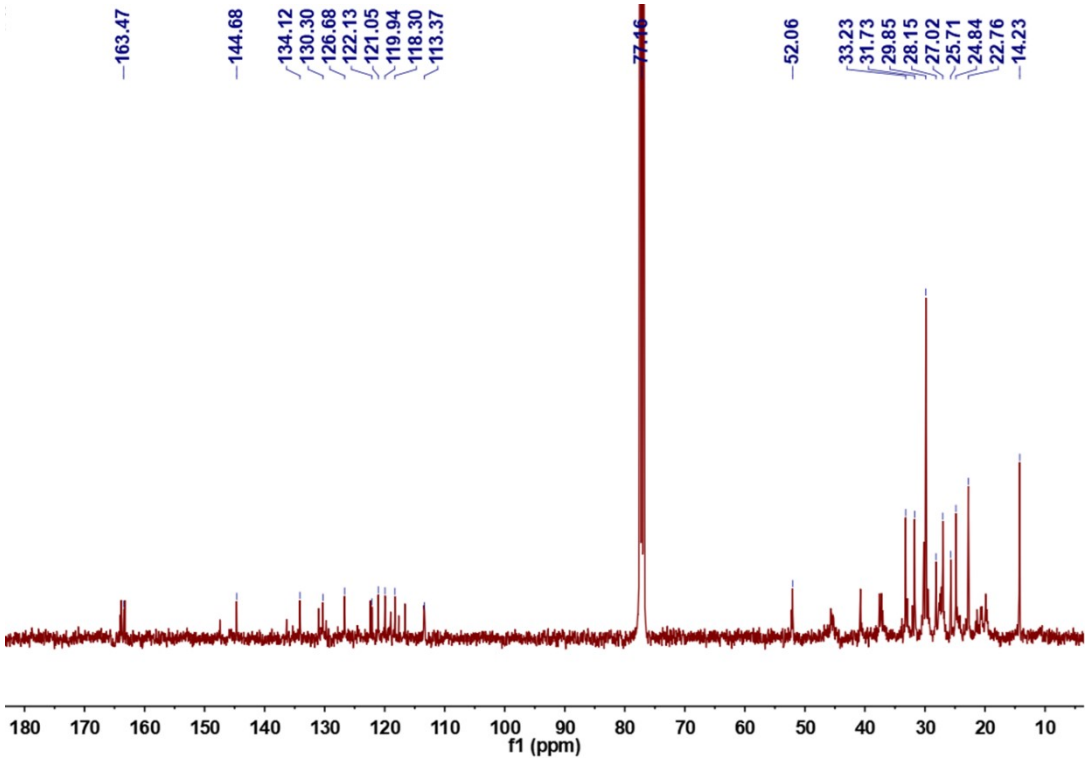

Fig. S4 ^{13}C NMR spectrum of compound **PDIA** in $CDCl_3$.

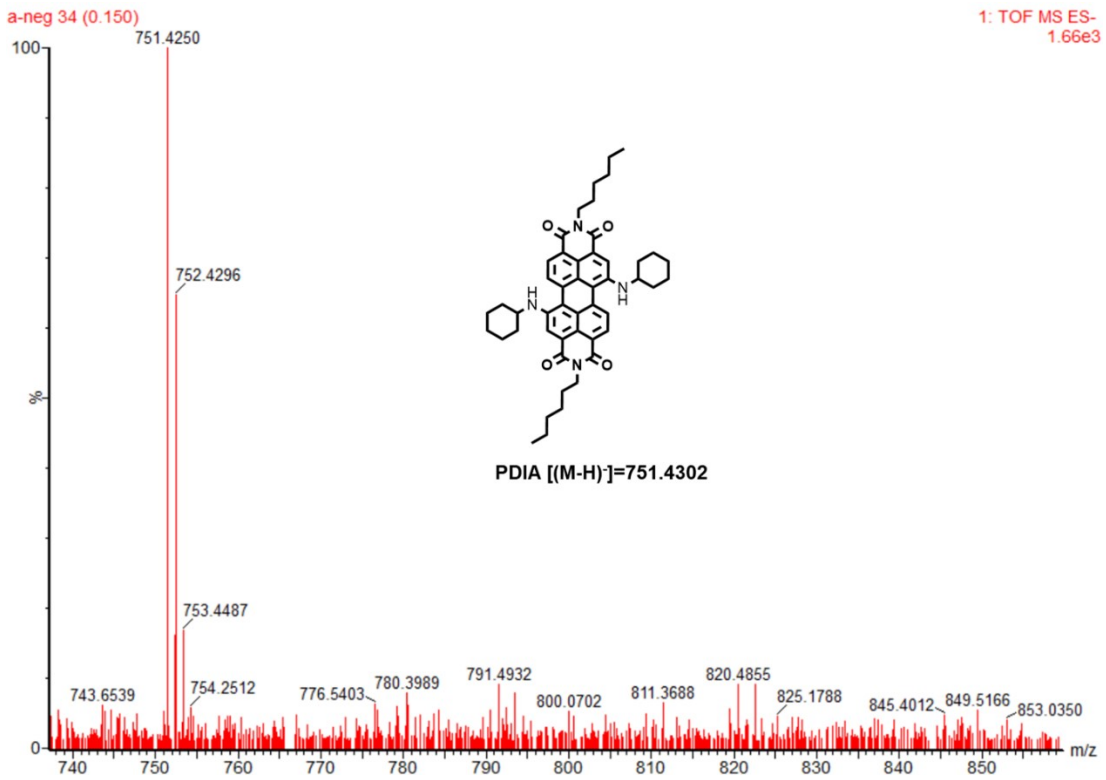

Fig. S5 Mass spectrum of compound **PDIA**.

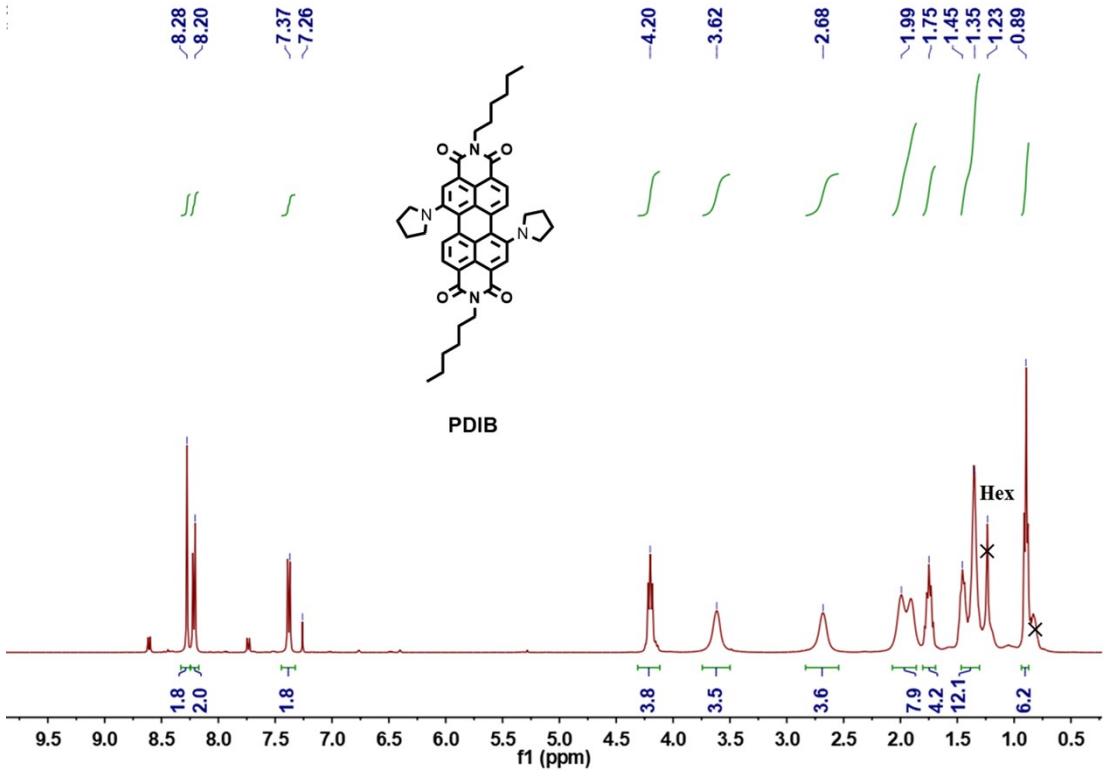

Fig. S6 ^{1}H NMR spectrum of compound **PDIB** in $CDCl_3$.

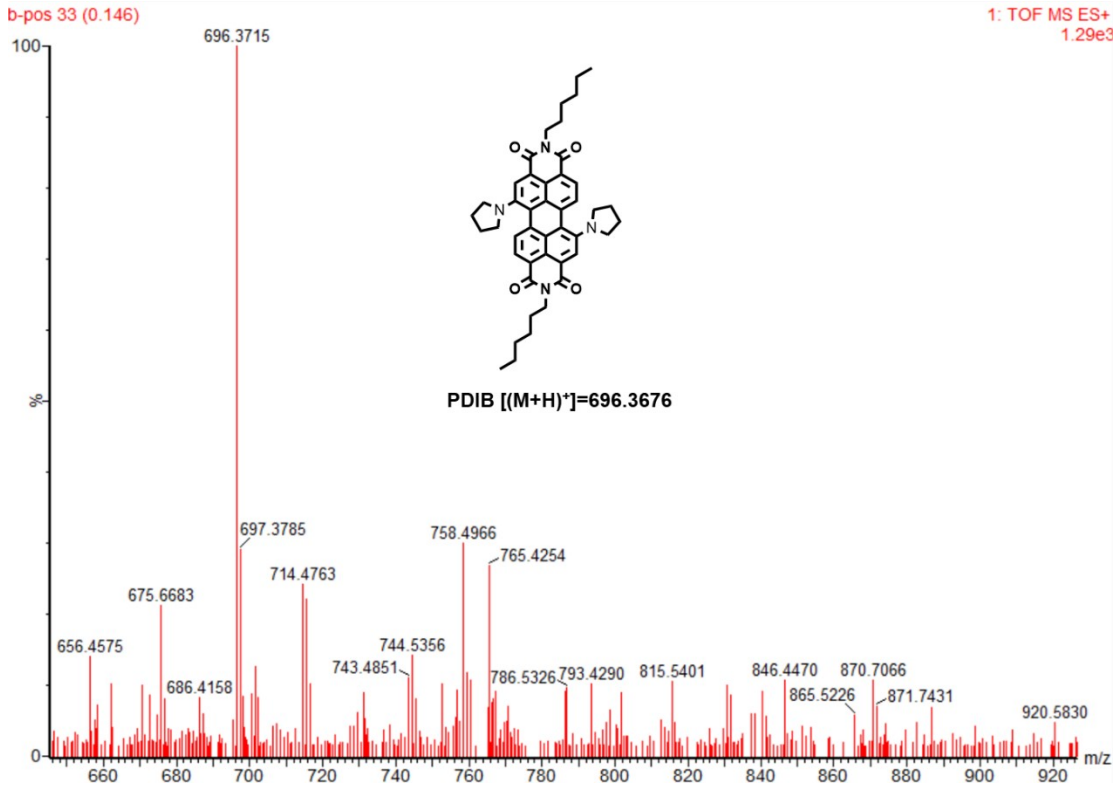

Fig. S7 Mass spectrum of compound **PDIB**.

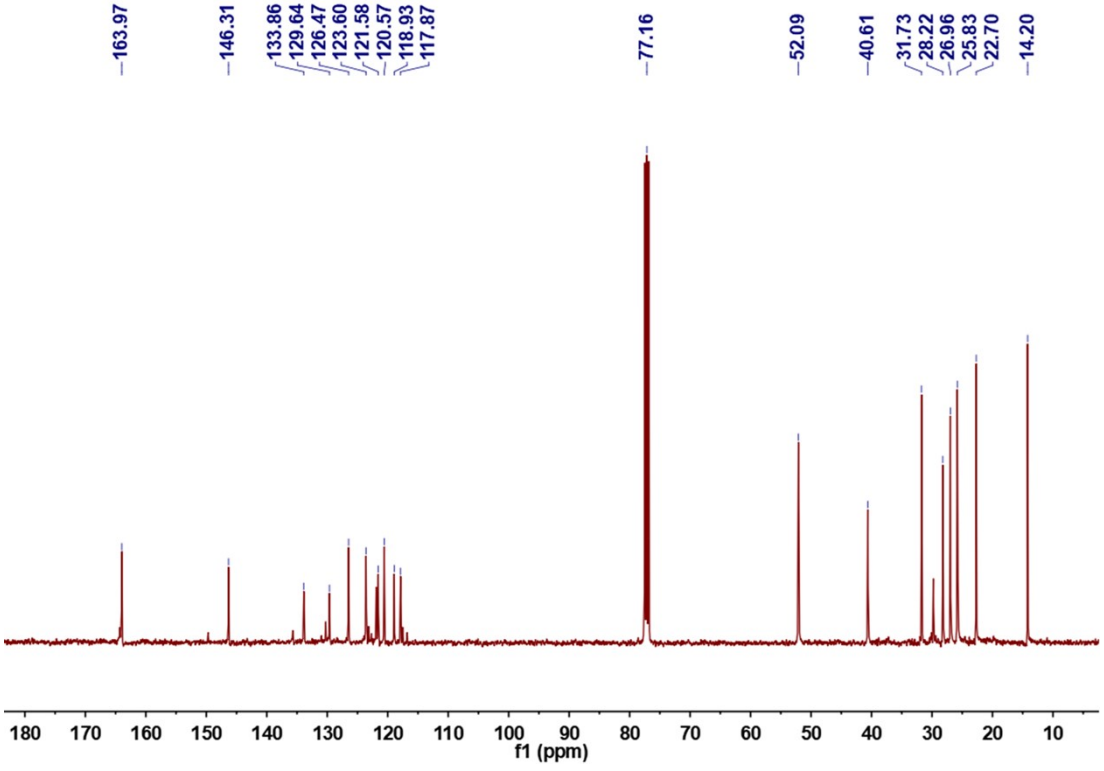

Fig. S8 ^{13}C NMR spectrum of compound **PDIB** in $CDCl_3$.

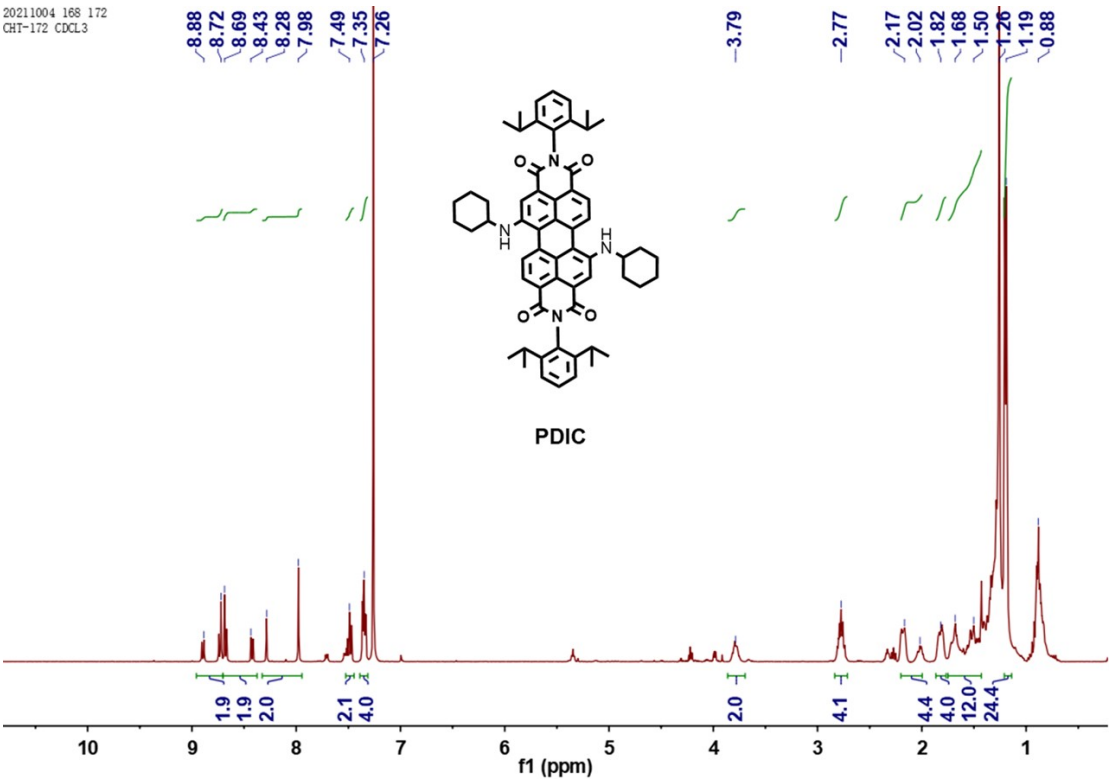

Fig. S9 ^{1}H NMR spectrum of compound **PDIC** in $CDCl_3$.

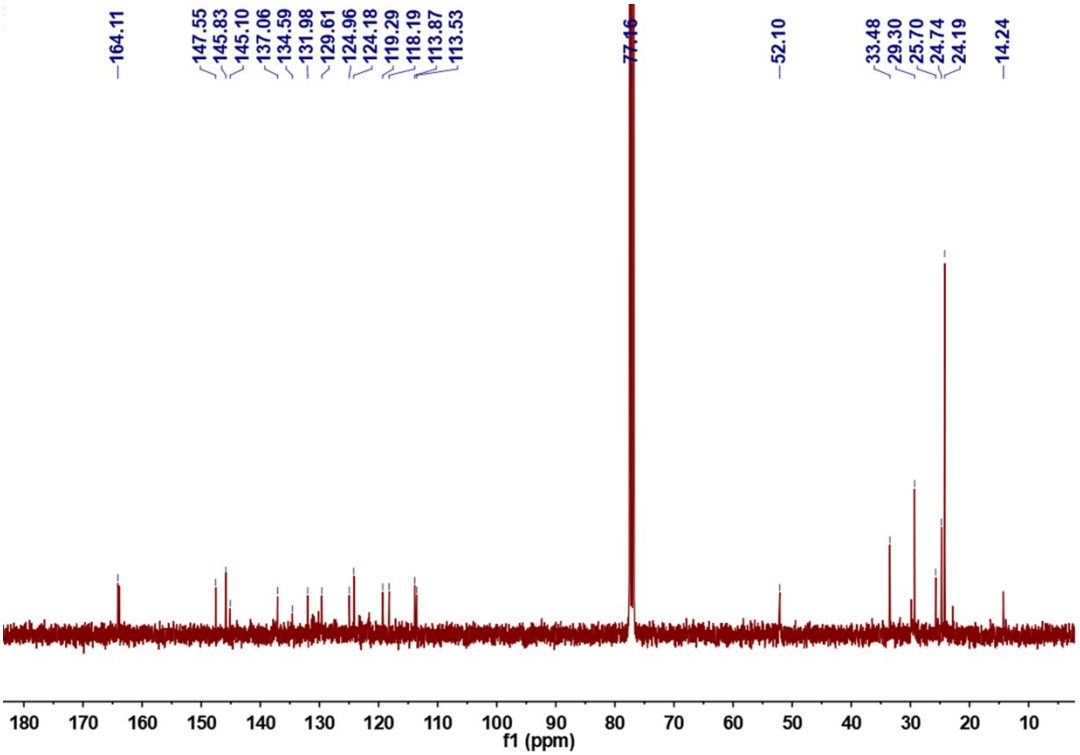

Fig. S10 ^{13}C NMR spectrum of compound **PDIC** in $CDCl_3$.

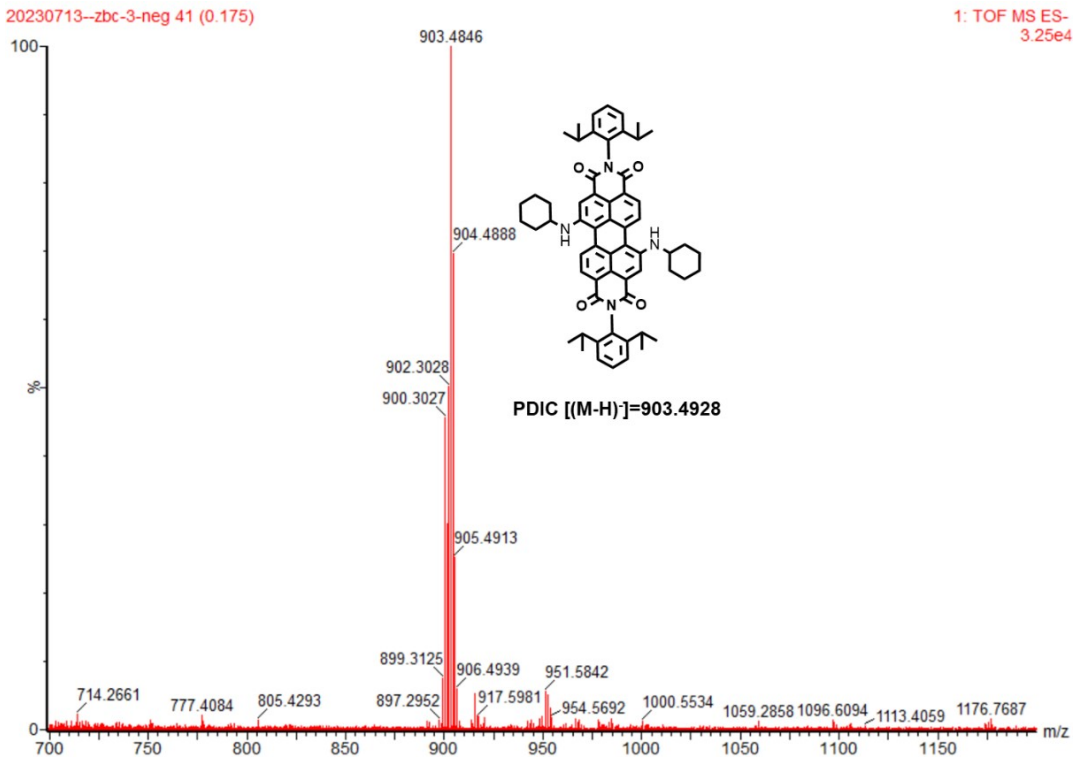

Fig. S11 Mass spectrum of compound **PDIC**.

Table S1 Properties of PDIA, PDIB, and PDIC in their monomeric and aggregated states.

Sample	PDIA monomer	PDIB monomer	PDIC monomer	PDIA aggregate	PDIB aggregate	PDIC aggregate
λ_{max} /nm	681	684	682	790	722	733
λ_{em} /nm	759	726	756	--	--	--
Red-shift /nm	--	--	--	109	38	51
ε /10^5 M^{-1} cm^{-1}	237.5	243.0	294.8	146.2	147.3	168.6
Q_Y	1.60%	28.38%	2.87%	--	--	--

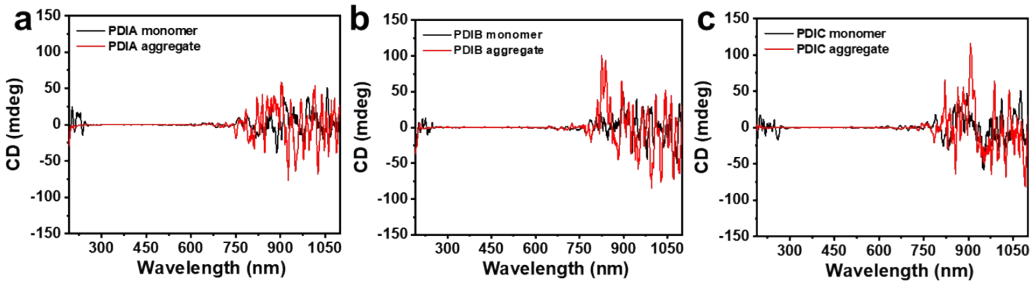

Fig. S12 The circular dichroism (CD) spectra of PDIA, PDIB, and PDIC.

No CD signals were observed in Fig. S12, which indicates that the formed aggregates did not exhibit any distinct secondary structures or specific chiral properties.

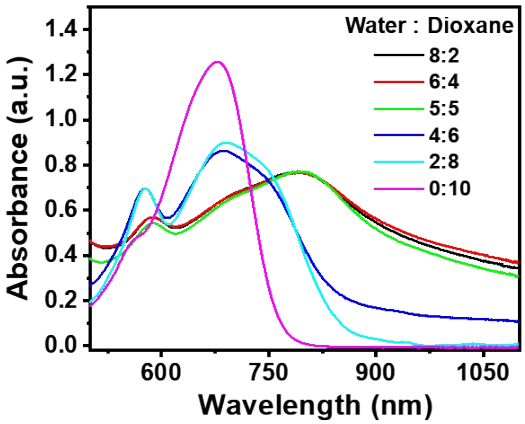

Fig. S13 The absorption spectra of PDIA with different water and dioxane ratio.

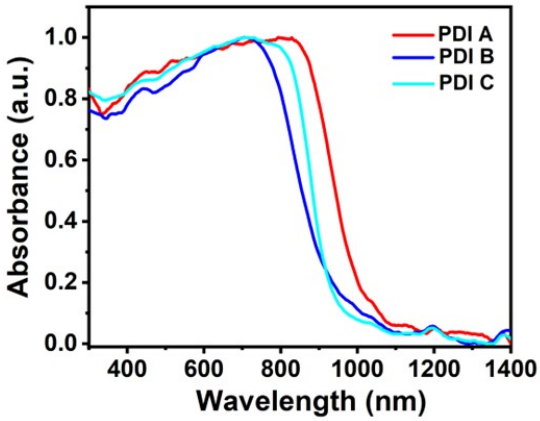

Fig. S14 Solid absorption spectra of PDIA, PDIB, and PDIC.

Theoretical calculation: The minimum energy structures of PDIA, PDIB, and PDIC monomers were calculated in the framework of density generalization using the B3LYP generalization function and 6-31G* basis set. All DFT calculations were performed using Gaussian distributions. For PDIA and PDIB, the long alkoxy (-OC_6H_{13}) chains were substituted with methyl groups to alleviate the computational cost. The PDIA, PDIB, and PDIC were

considered to be the most stable conformations as shown in Fig. S13.

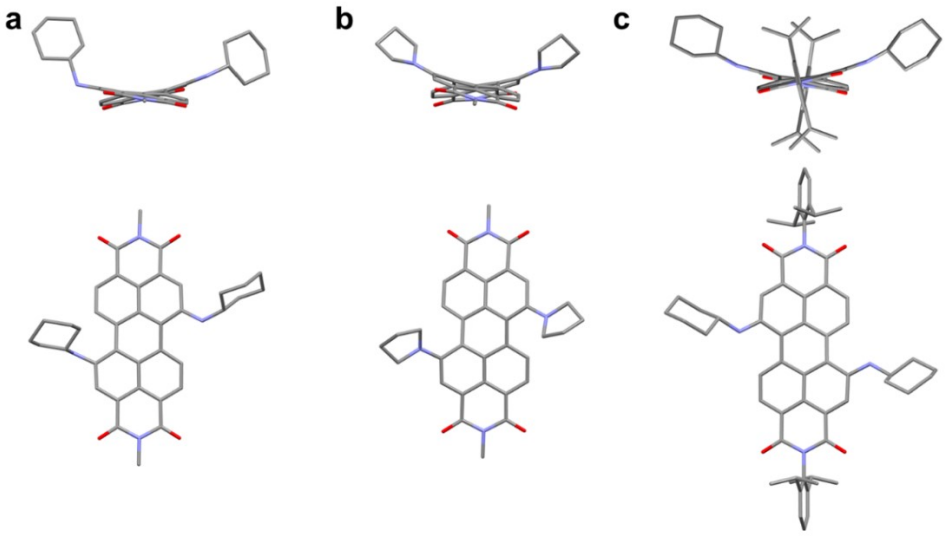

Fig. S15 Optimized geometries and molecular packings by molecular dynamics simulation. Minimum-energy structures are computed at the B3LYP/6-31G* level for the most stable conformers of PDIA, PDIB, and PDIC.

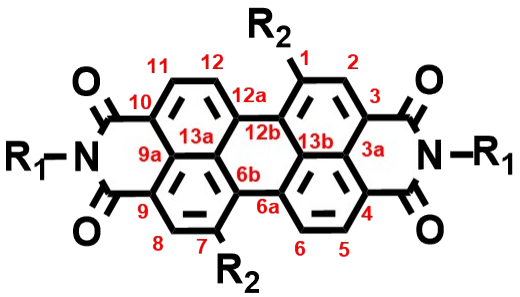

Fig. S16 Chemical structure of the PDI with labeling of the carbon atoms of the chromophore core (red).

Table S2 Structural parameters of PDIA, PDIB, and PDIC.

Sample	Core twist [a] [°]	Θ(C1-C12b-C12a-C12) [b] [°]	Θ(C6-C6a-C6b-C7) [b] [°]
PDIA	21.25 [c]	22.10	15.97
PDIB	28.75	20.87	20.91
PDIC	22.62	21.79	21.57

a) Angle between the PDI's two naphthalene subunits;

b) Numbering of carbon atoms are according to Fig. 16;

c) Based on the optimized geometry and molecular fillers of molecular dynamics simulations (Fig. S16), we measured the angles between the plane with Mercury.

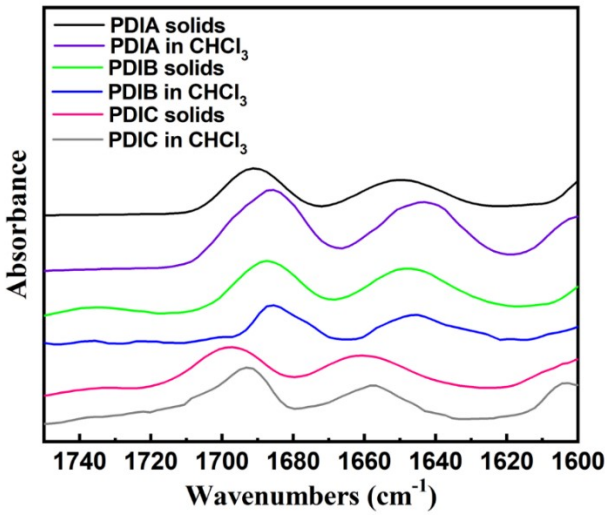

Fig. S17 Fourier-transform infrared spectroscopy of PDIA, PDIB, and PDIC.

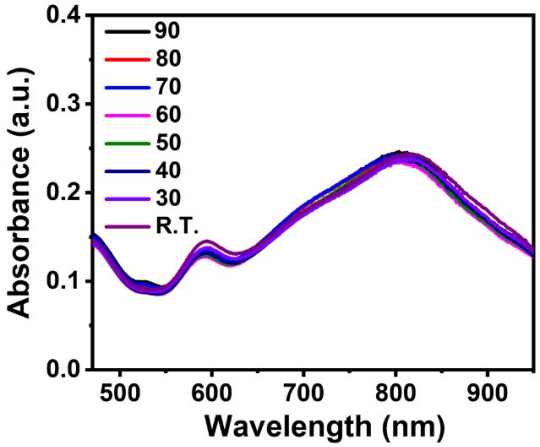

Fig. S18 The absorption spectra of PDIA solution increased from room temperature to 90 °C.

3. Assembly Study of PDIA, PDIB, and PDIC

To overcome the hydrophobicity and obtain a small size of PDI J-aggregates, we examined the influence of conditions during PDIs assembly (solvent types, mixed mode, and surfactant types) by comparing the absorption spectra and size of assemblies (Table S3).

Condition 1: (1) PDIA (2 mg) and DSPE-PEG (10 mg) were mixed in 1 mL of DMF. The mixture was stirred for 10 min to ensure complete dissolution of the components.

(2) A 10 mL glass test tube containing 4 mL of deionized water was prepared. The water was vigorously stirred at a speed of 1400 rpm. The DMF solution obtained in step (1) was then added dropwise within 30 min, and stirred for another 30 min;

(3) The resulting mixture from step (2) was transferred into a dialysis bag with a molecular weight cutoff (MWCO) of 3500. The dialysis bag containing the mixture was immersed in water, and the water was replaced every 8 h for a total duration of 24 h.

Condition 2: The method was identical to condition 1, with the only difference of replacing DMF with dioxane.

Condition 3: (1) PDIA (2 mg) and DSPE-PEG (10 mg) mixed in 1 mL of dioxane. The

mixture was stirred for 10 min to ensure complete dissolution of the components.

(2) A 10 mL glass test tube containing the dioxane solution obtained in step (1) was prepared. The solution was vigorously stirred at a speed of 1400 rpm. The 4 mL deionized water was then added dropwise within 30 min, and stirred for another 30 min;

(3) The resulting mixture from step (2) was transferred into a dialysis bag with a molecular weight cutoff (MWCO) of 3500. The dialysis bag containing the mixture was immersed in water, and the water was replaced every 8 h for a total duration of 24 h.

Condition 4: The method was identical to condition 3, with the only difference of replacing F127 with DSPE-PEG.

Table S3 Process conditions of PDIA assemblies.

Condition	**1**	**2**	**3**	**4**
Surfactant	DSPE-PEG_{2000}	DSPE-PEG_{2000}	DSPE-PEG_{2000}	F127
Good solvent	DMF	Dioxane	Dioxane	Dioxane
Mixed mode	Solution to water	Solution to water	Water to solution	Water to solution

Table S4 Properties of PDIA assemblies under different conditions.

Condition	**1**	**2**	**3**	**4**
λ_{max} / nm	695	689	787	785
Red-shift / nm	14	8	106	104
Size / nm	292	59	129	191

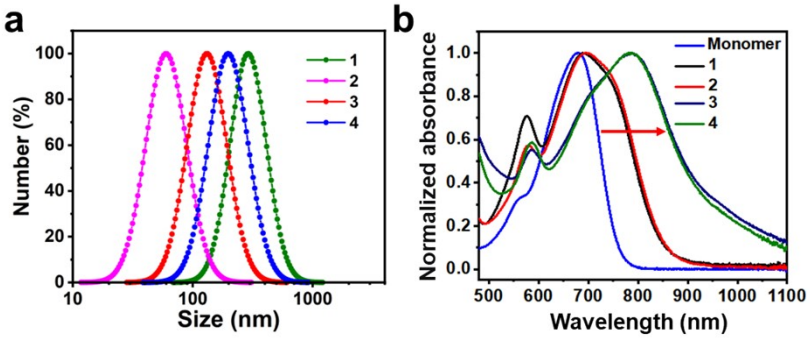

Fig. S19 (a) DLS size and (b) Absorbance spectra of PDIA assemblies in different conditions.

The effects of solvent type, mixed mode, and polymer type on absorption wavelength and particle size were investigated (Table S3). Compared to DMF, using dioxane as the good solvent resulted in an average assembly size of less than 200 nm. The mixed mode was also examined. Whether adding the dioxane solution to water or adding water to

dioxane, the average size of the assembly remained below 200 nm (Fig. S19a and Table S4). Furthermore, substituting the surfactant DSPE-PEG with F127 still resulted in red-shift of over 100 nm in the absorption, but the size of the aggregates obtained was much larger, reaching close to 200 nm (Fig. S19b and Table S4). Therefore, the assembly formed by adding water to the dioxane solution of PDIA and DSPE-PEG (Condition 3) was selected for subsequent investigations.

Table S5 Properties of different PDI assemblies.

Sample	PDIA	PDIB	PDIC
λ_{max} (monomer)	681	684	682
λ_{max} (aggregation)	787	715	737
Red-shift /nm	106	31	55
Size /nm	131	153	183

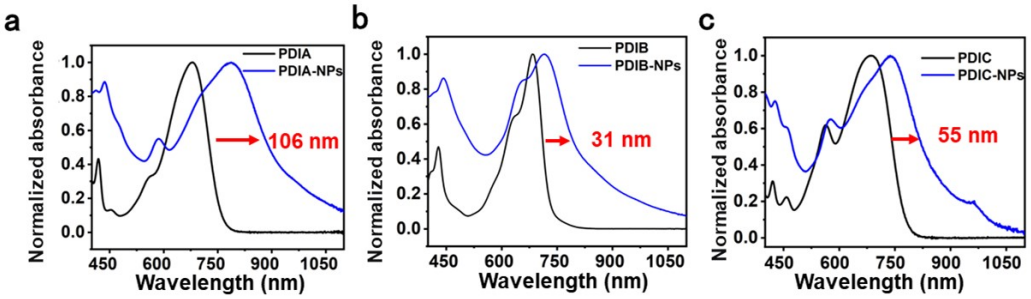

Fig. S20 Absorbance spectra of (a) PDIA-NPs, (b) PDIB-NPs, and (c) PDIC-NPs.

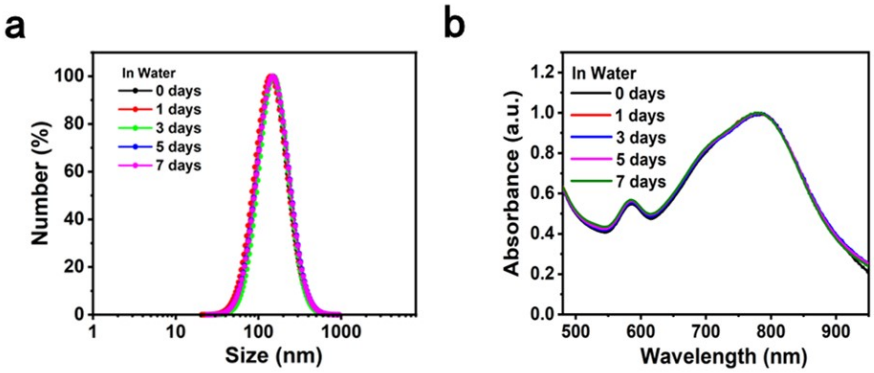

Fig. S21 (a) Size changes of PDIA-NPs during storage measured by DLS at 25 °C in aqueous solutions. (b) Absorption spectra of PDIA-NPs during storage in aqueous solutions.

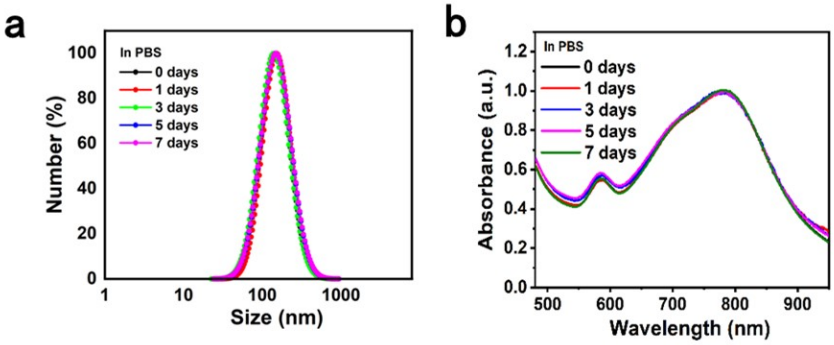

Fig. S22 (a) Size changes of PDIA-NPs during storage measured by DLS at 25 °C in PBS solutions. (b) Absorption spectra of PDIA-NPs during storage in PBS solutions.

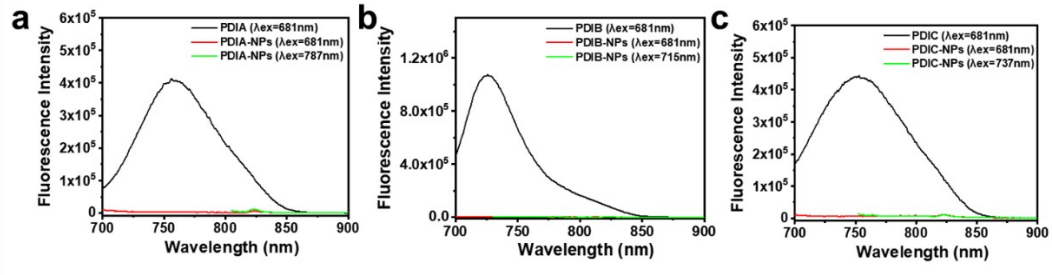

Fig. S23 Fluorescence emission spectra of the solutions of PDIA, PDIB, and PDIC in dioxane and PDIA-NPs, PDIB-NPs, and PDIC-NPs in water.

The generation of singlet oxygen was evaluated by monitoring the change in absorption of 1,3-diphenylisobenzofuran (DPBF), which serves as a singlet oxygen sensor. The absorption of DPBF at 410 nm was measured during NIR laser irradiation with different times of exposure. Specifically, the NIR laser irradiation wavelengths used were 660 nm for PDIA and 808 nm for PDIA-NPs.

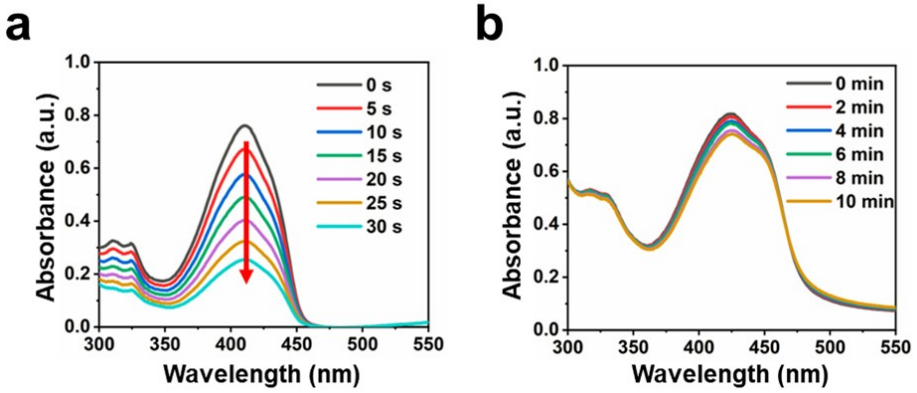

Fig. S24 Time-dependent absorption spectra changes were seen for 100 μM DPBF and 20 μM PDIA-NPs in (a) acetonitrile solutions, and (b) aqueous solution under laser irradiation (a: 0.05 W/cm^2, 660 nm; b: 0.2 W/cm^2, 808 nm).

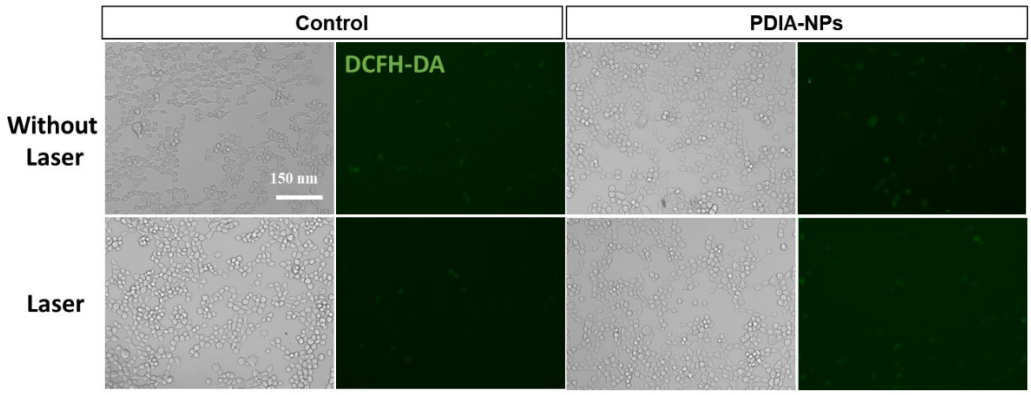

Fig. S25 Intracellular generation of ROS after different treatments with DCFH-DA as a probe with or without laser irradiation (808 nm, 0.5 W/cm^2, 10 min).

4. Photothermal performance

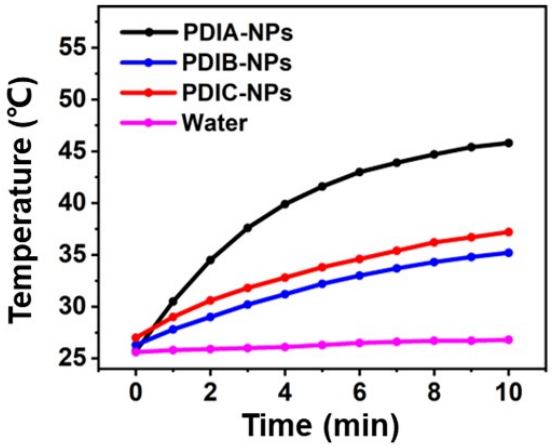

Fig. S26 Temperature changes of PDIA-NPs, PDIB-NPs, and PDIC-NPs in water upon 808 nm laser irradiation for different time intervals.

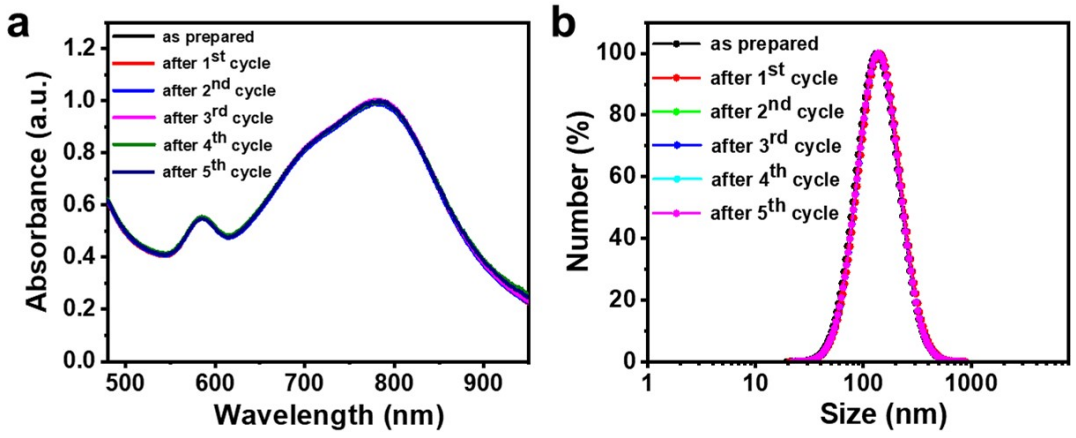

Fig. S27 (a) The absorption spectra and (b) size of PDIA-NPs during five circles of heating-cooling processes.

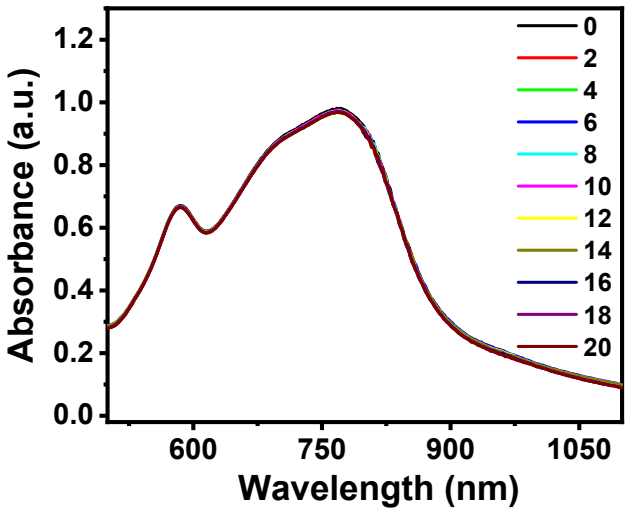

Fig. S28 The absorption spectra of PDIA-NPs during laser irradiation within 20 min.

Detection of photothermal effect. PDIA-NPs (0, 10, 20, 50, 100, and 200 μg/mL) in water were put into a cuvette and exposed to 808 nm laser (1.0 W/cm^2) for 10 min respectively. The IR imaging and temperature data were recorded by a Fluke (Ti400) thermal imaging camera.

Photothermal conversion efficiency test. PDIA-NPs was put into a cuvette and exposed to an 808 nm laser at 0.5 W/cm^2. When the temperature reaches to maximum steady state, the PDIA-NPs cooled down naturally after the laser shut off. During the procedure, the temperature was recorded by the thermal imaging camera. The photothermal conversion efficiency (η) was calculated:

$$\eta = \frac{h_A\left(T_{max} - T_{sur}\right) - Q_s}{I(1 - 10^{-A})}$$

where h is the heat transfer coefficient, A is the surface area of the container, T_{max} is the maximum steady-state temperature, T_{sur} represents the ambient temperature of the environment, Qs is the heat dissipation of solvent (water) which was measured by a power meter (407A, Spectra-Physics), I is the incident laser power (0.5 W/cm^2), and A is the absorbance of the PDIA-NPs at 808 nm. h_A was calculated by the following equation:

$$h_A = \frac{\sum m_i C_i}{\tau_s}$$

where m_i and C_i are the mass (1 g) and heat capacity (4.2 J/g) of water, respectively.
τ_s is the sample system time constant calculated by the following equation:

$$\tau_s = -\frac{t}{\ln \theta}$$

where t represents time. θ is the dimensionless driving force defined as $(T\text{-}T_{sur})/(T_{max}\text{-}T_{sur})$.

5. Cellular studies

Cell viability test by CCK-8 assay. Mouse mammary carcinoma cell line 4T1 cells in the growth of log phase were cultured in a 96-well plate at the density of ~6000 cells/well and incubated for 24 h. Various concentrations of PDIA-NPs in culture media were added to each

well (100 μL/well). After 24 h or 48 h exposure to PDIA-NPs, the culture media were changed back to fresh culture media and cell viability was tested by Standard CCK-8 assay.

Live/dead cell staining. 4T1 cells in the growth of log phase were cultured in a 96-well plate at the density of ~6000 cells/well and incubated for 24 h. Various concentrations of PDIA-NPs in culture media were added to each well (100 μL/well) for 24 h incubation. The treated cells were exposed to laser irradiation (808 nm, 0.5 W/cm^2, 10 min). Cell viability after PTT was investigated by Standard CCK-8 assay. After photothermal treatment, the four groups, cells with PBS, only PDIA-NPs, only laser, and PDIA-NPs with laser, were co-stained with Calcein-AM and PI, and monitored by EVOS® FL Auto Cell Imaging System.

Cellular ROS Generation Assay. The intracellular ROS production was measured by dichlorofluorescein diacetate (DCFH-DA). 4T1 cells were incubated in 96-well plates for 24 h with a density of 5000 cells per well containing complete DMEM media for 24 h. Then, the 4T1 cells were incubated with PBS, and PDIA-NPs for 4 h with or without 808 nm laser irradiated (10 min, 0.5 W/cm^2). The cells medium was replaced with the fresh DMEM containing DCFH-DA solution at the concentration of 10×10^{-6} M for 20 min and washed three times with PBS. Then, the cells were observed by fluorescence microscopy to evaluate the ROS generation. The excitation wavelength and emission wavelength were 485 nm and 525 nm, respectively.

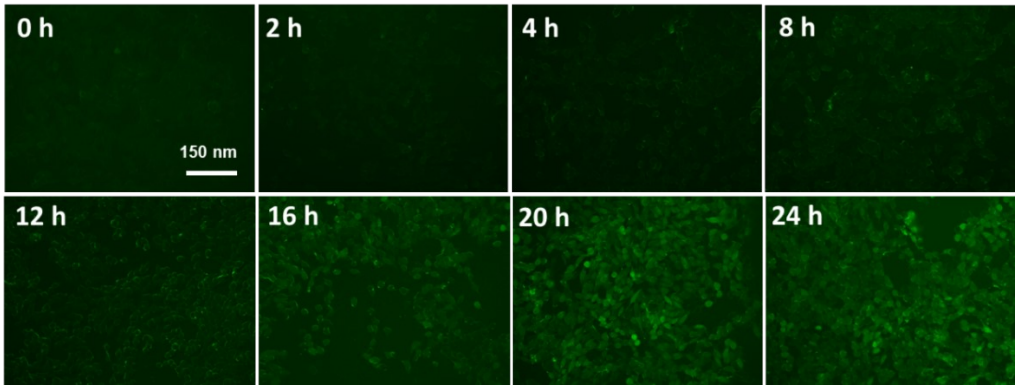

Fig. S29 Fluorescence images of 4T1 cells after incubation with FITC-PDIA-NPs for different time.

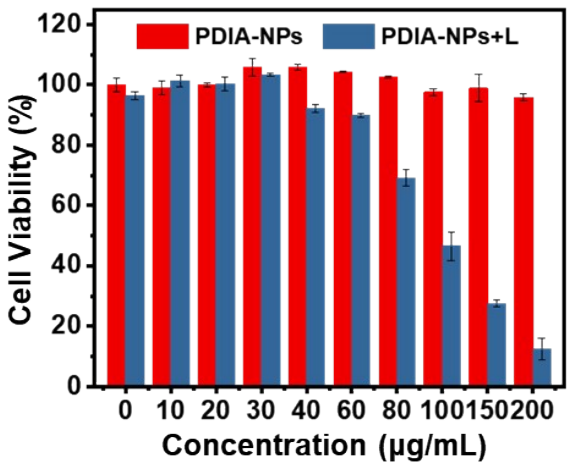

Fig. S30 Cell viabilities of HUVECs incubated with PDIA-NPs with/without laser irradiation, as determined by CCK-8 assay.